ELSEVIER

Contents lists available at ScienceDirect

Analytica Chimica Acta

journal homepage: www.elsevier.com/locate/aca





DNA hydrogels combined with microfluidic chips for melamine detection

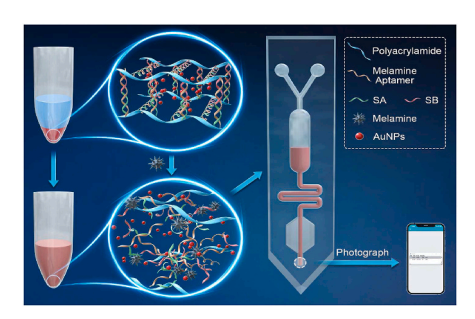
Zhiguang Wang ^{a,b}, Ruipeng Chen ^b, Yue Hou ^{a,b}, Yingkai Qin ^b, Shuang Li ^{b,*}, Shiping Yang ^{a,**}, Zhixian Gao ^{b,***}

- ^a College of Chemistry and Materials Science, Shanghai Normal University, Shanghai, 200234, China
- ^b Tianjin Key Laboratory of Risk Assessment and Control Technology for Environment and Food Safety, Institute of Environmental and Operational Medicine, Tianjin, 300050, China

HIGHLIGHTS

- A specific colorimetric detection method for melamine using AuNPs - encapsulated DNA hydrogel was constructed.
- A POCT detection platform is prepared by combining microfluidic chip.
- The POCT platform can detect melamine with a detection limit to 37 nM.
- By changing the aptamer in DNA hydrogel, this strategy can be used to detect other targets.

GRAPHICAL ABSTRACT



ARTICLE INFO

Keywords: DNA hydrogel Microfluidic chip Melamine detection

ABSTRACT

The illegal addition of melamine (MEL) into pet foods and infant milk powder has caused great concern among people. In this study, a point-of-care testing (POCT) method was developed by combining stimuli-responsive deoxyribonucleic acid (DNA) hydrogels with microfluidic chips to achieve portable and sensitive detection of MEL. With the MEL aptamer (MA) acting as a cross-linker, DNA hydrogel-coated gold nanoparticles (AuNPs) served as a basis for colorimetric detection and quantitative analysis. In the presence of MEL, it competitively binds to the aptamer, causing disintegration of the DNA hydrogels and a release of the coated AuNPs, making it possible to visually detect and quantitatively measure the MEL. Under optimal conditions, the detection range of MEL using DNA hydrogels was 0.1-100 μM and the limit of detection (LOD) was 42 nM. This portable, sensitive, and user-friendly field test equipment was developed to avoid the use of non-portable laboratory instruments. Furthermore, we combined microfluidic chips with the properties of DNA hydrogels, making it possible to quantitatively detect MEL by taking photos and analyzing the gray value using software in accordance with the different colors of copolymerization solutions after the reaction. The detection range of MEL using the microfluidic chip-based method was 0.2-50 µM, and the LOD was 37 nM. Neither trained operators nor large-scale instruments are needed for using this method to conduct portable and sensitive field detection of the targets, which highlights the methods excellent potential in food security, clinical tests, environmental monitoring, and other aspects.

E-mail addresses: liza3320@163.com (S. Li), shipingy@shnu.edu.cn (S. Yang), gaozhx@163.com (Z. Gao).

^{*} Corresponding author.

^{**} Corresponding author.

^{***} Corresponding author.

1. Introduction

Melamine (MEL) is one of the raw materials used for the production of plastics, coatings, and adhesives [1]. Owing to its high nitrogen content, MEL is added to dairy products and animal feed to increase the apparent protein content [2] as determined by the Kjeldahl method that is usually adopted to determine the protein content in foods or feed. The illegal addition of MEL led to pet food contamination in the United States in 2007 and infant milk powder adulteration in China in 2008 [3], Research indicates that intake of MEL causes lithiasis and other illnesses in animals and infants [4,5]. MEL is classified as a group 2B carcinogen by the International Agency for Research on Cancer (IARC). United Nations Food Standards Commission set a safe limit of MEL in foods at 2.5 mg L^{-1} (19.8 μ M) and in infant milk powder at 1 mg L^{-1} (7.9 μ M), and therefore, MEL detection has attracted increasing attention from researchers.

Traditional MEL detection methods, including liquid chromatography, gas chromatography, gas chromatography mass spectrometry, and atomic absorption spectrographic method [6] require expensive large-scale instruments, strict pretreatment of samples, and highly skilled operators. With the advantages of high sensitivity, low limit of detection (LOD), and simple processing, nanotechnology-based detection methods have greatly helped to advance the development of rapid detection technologies to overcome the shortcomings of traditional technologies in MEL detection.

Hazra et al. achieved sensitive detection of MEL based on the selective quenching of the luminescence signal of upconversion nanocrystals by melamine [7]. Liao et al. opened and closed the fluorescence signals of β -cyclodextrin modified carbon nanoparticles by replacing Fe³⁺ with MEL [8] and obtained outstanding results for MEL detection in milk. Xie et al. prepared microfluidic paper-based analytical devices (μPADs) based on gold nanoparticles (AuNPs) [9] to implement a low-cost, portable, and sensitive method for the detection of MEL, which is therefore highly suitable for use in regions with limited resources. Among the various detection methods, point-of-care testing (POCT) methods has the advantages of fast detection, simple use and saving comprehensive cost appeal to the author. Common POCT technologies include lateral flow immunoassays (such as virus test paper [10]), sensor technology (such as glucometer [11]), and microfluidic technology [12], which have grown rapidly in recent years. Microfluidic chips have been widely applied to POCT detection platforms owing to their advantages of low cost and transformation of different signals [13-16]. Compared to conventional quantitative analysis, colorimetric detection in POCT allows for both real-time qualitative and semiquantitative analyses without relying on any advanced or complex instruments. It is worth noting that AuNPs have been favored by researchers in the application of colorimetric detection for a long time because of their mature synthetic technology and stability [17]. To achieve the goal of both colorimetric and quantitative detection and develop a user-friendly POCT detection platform, deoxyribonucleic acid (DNA) hydrogels were combined with microfluidic chips in this study. As a result, colorimetric detection was possible based on the color of the copolymerization solutions after the reaction, and quantification could also be carried out simply by analyzing the gray value with specific software instead of using large-scale instruments.

Stimuli-responsive DNA hydrogels possess both the programmability of DNAs and the good bearing capacity of hydrogels [18], and therefore receive increasing attention in the development of biosensors. The rational design and precise application of DNA strands enable hydrogels to have greater responsiveness, including responsiveness to non-biological (light [19], heat [20], magnetism [21], pH [22], etc.) and biological stimuli (nucleic acids [23], proteins [24], small molecules [25], etc.). Generally, a specific response to the target can be achieved by introducing the nucleic acid aptamer into hydrogels. The nucleic acid aptamer can be separated using systematic evolution of ligands by exponential enrichment (SELEX) technology, and the nucleic acid

aptamer have the advantages of a wide target range, massive scale *in vitro* synthesis, great repeatability, high stability, and low cost [26]. The MEL aptamer (MA) adopted in this study was modified from the aptamer obtained by Gu et al. using SELEX [27], and displayed good affinity and better selectivity. This detection platform has potential for further application in the portable and quantitative detection of other targets by altering the aptamer used in the system.

In this study, a portable and sensitive POCT detection platform was designed, in which aptamer-based stimuli-responsive DNA hydrogels are combined with microfluidic chips, enabling the sensitive detection of MEL. First, AuNPs were encapsulated in polyacrylamide DNA hydrogels bridged by MA. Next, these complexes competitively bind to the aptamer in the presence of MEL, which leads to hydrogel rupture and AuNPs release. The AuNPs used in this method provide a basis for the colorimetric and quantitative detection of the targets. In this case, microfluidic chips were introduced to construct a POTC detecting platform for immediate analysis at the sampling site. The DNA hydrogels did not flow directly from the reaction area to the lower detection area. however, following the completion of the reaction, the copolymerization solutions did flow into the detection area under gravity. At that time, photos were taken using mobile phones and the gray value was analyzed using ImageJ software to perform a quantitative analysis of the detected concentrations. The target concentration was positively correlated with the amount of AuNPs released by the DNA hydrogels and negatively correlated with the gray value. The POCT detection equipment showed a lower LOD of 37 nM for MEL. As a result of this study, we developed a portable, inexpensive, and simple to operate detection platform for quantitative analysis, which does not depend on large-scale laboratory instruments.

2. Materials and methods

2.1. Materials and reagents

Ammonium persulfate (APS), N,N,N',N'-Tetramethylethylenediamine (TEMED), and Tris-hydrogen chloride (HCl) buffer were purchased from Shanghai Acmec Biochemical Co., Ltd. (Shanghai, China). MEL, glucose, sucrose, lysine, L-cysteine, histidine, adenine, and thymidine were obtained from Alta Scientific Co., Ltd. (Tianjin, China) and had a purity of over 99%. All other reagents were acquired from Sigma-Aldrich (St. Louis, MO, USA). All oligonucleotide sequences were purified by high-performance liquid chromatography (HPLC) and synthesized by Sangon Biotechnology Co., Ltd. (Shanghai, China). Oligonucleotide sequences are listed in Table S1.

2.2. Apparatus and characterization

Absorbance was measured using ultraviolet and visible spectrophotometry (UV-vis, TU-1901, Persee Co., Ltd., China). DNA hydrogels were subjected to freeze-drying (Freeze dryer, SCIENTZ-10ND, Scinetz, China) and their morphological characteristics were observed using scanning electron microscopy (SEM, ZEISS Sigma 300, Germany). Transmission electron microscopy (TEM, Tecnai G2 F20 S-TWIN, FEI, USA) and a dynamic/static laser scattering instrument (DLS, Zetasizer Nano ZSE, UK) were used to analyze whether the synthesized AuNPs qualified. Circular dichroism (CD, CHIRASCAN, Applied Photophysics Ltd, UK) and electrophoresis (DYY-11, Liuyi Instrument Factory, China) were also used in this experiment.

2.3. Synthesis of AuNPs

AuNPs were synthesized according to the method reported previously [28], using glassware that had been immersed in aqua regia (HCl: $\rm HNO_3=3:1,\,v/v)$ for 120 min, washed with ultrapure water and dried. Briefly, 100 mL of 0.01% (w/v) HAuCl₄ was boiled in a 250-mL round-bottom flask and quickly added to 2.6 mL of 1% freshly

prepared sodium citrate solution (Na $_3$ C $_6$ H $_5$ O $_7\cdot$ 2H $_2$ O). Next, the resulting mixture was boiled and stirred for 30 min to obtain an AuNP solution with a concentration of 2.5 nM and a particle size of 15 nm. Finally, polyethylene glycol thiol (PEG-SH, Mw 5000) was added to modify the AuNPs and 0.01 wt% Tween-20 was used as a coating to avoid coagulation. The obtained AuNPs were centrifuged and redispersed to the required concentration. The characterization of the synthesized AuNPs is shown in Fig. S1. The TEM image shows that the particle size of the synthesized AuNPs is 15 nm and well dispersed. The hydrated particle size of AuNPs is further analyzed by dynamic light scattering (DLS) analysis, and the results are slightly larger than the TEM results.

2.4. Preparation of DNA hydrogels

First, the linear polyacrylamide-DNA polymer was prepared by modifying from previous studies [29]. Specifically, SA or SB was mixed with 2.4% acrylamide in an Eppendorf tube and homogenized by shaking, followed by vacuum deoxidation at 37 $^{\circ}\text{C}$ for 6 min. Subsequently, 1.4% APS (freshly prepared, 10 wt%) and 2.8% TEMED (freshly prepared, volume ratio of 5%) were added and blended, followed by vacuum deoxidation at 37 $^{\circ}\text{C}$ for 8 min to synthesize the P-SA or P-SB polymer. The P-SA or P-SB generated (SA or SB with a final concentration of 100 $\mu\text{M})$ was centrifuged and purified using ultrafiltration centrifuge tubes with a molecular weight of 100 KD so as to remove unpolymerized monomers and polymers with a low molecular weight.

Thereafter, MEL-responsive DNA hydrogels were prepared as follows. First, 6 μL of AuNPs, 5 μL of P-SA, and 5 μL of P-SB were mixed in Tris-HCl buffer and vigorously shaken for 5 min at 60 °C. Then, 5 μL of MA (denatured at 95 °C and slowly cooled down to room temperature) at a certain concentration was added and shaken thoroughly for 10 min at 60 °C. As the samples were slowly cooled to room temperature, the DNA hydrogels were washed three times with Tris-HCl buffer to remove AuNPs on the surface of the polymers. The prepared DNA hydrogels were stored overnight at room temperature to ensure complete cross-linking between the DNA molecules.

2.5. Ultraviolet detection of MEL

For ultraviolet detection, 75 μ L of MEL standard solutions with a series of concentrations were added to DNA hydrogels, and the reaction was carried out by incubation at 37 °C and 150 rpm for 1 h, resulting in a change of color of the supernatant. The absorbance of the supernatant was measured to obtain precise results.

2.6. Specificity analysis

To validate the response specificity and anti-interference ability of DNA hydrogels, substances that might co-exist with MEL or be destructive to DNA hydrogels were selected, including glucose, sucrose, lysine, L-cysteine, histidine, adenine, thymidine, Pb $^{2+}$, and Al $^{3+}$. According to the detection as per the aforementioned experimental procedures for MEL detection, the concentration of these substances was $100~\mu M$. In addition, they were compared to MEL at a concentration of $10~\mu M$. The absorbance of the supernatant was measured after the completion of the reaction.

2.7. Real sample analysis

To verify the detection capability of DNA hydrogels in actual samples, milk and infant milk powder samples were purchased from local supermarkets. After through pretreatment, different amounts of MEL were added, followed by detection as described above.

2.8. Design and detection of microfluidic chips

After drawing patterns using AutoCAD software, microfluidic chips

were prepared by Suzhou Shuotian Automation Technology Co., Ltd. (Suzhou, China) with polydimethylsiloxane (PDSM) upon receiving the patterns. The liquid storage, reaction area, liquid channel, and detection area were divided on the chips (Fig. S2). When DNA hydrogels and different concentrations of MEL solution were successively injected into the reaction area of the chips, the unreacted DNA hydrogels blocked the liquid channel. The analysis time of microfluidic chip is 60min, referring to the previous reaction time of DNA hydrogel and MEL. After the reaction, the chips were inclined to allow the sample solutions to flow through the liquid channel to the lower detection area. The detection area of the chips was photographed using a mobile phone camera, and the photos were imported to the ImageJ software (NIH, Bethesda, MD, USA) to analyze the average gray value.

3. Results and discussion

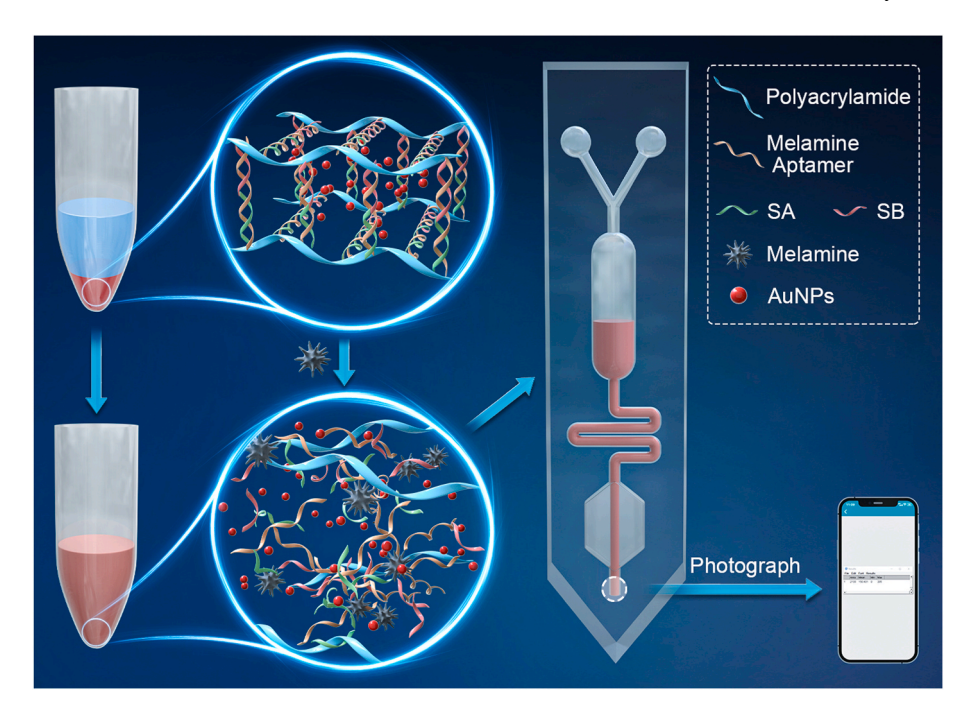
3.1. Experimental principles

The target-responsive DNA hydrogels synthesized for MEL detection, combined with microfluidic chips, are shown in Scheme 1. In brief, two sets of single-stranded DNAs (SA and SB) complementing part of the MA region were designed according to MA and grafted onto the polyacrylamide to form polymer chains (P-SA and P-SB). Next, MELresponsive DNA hydrogels were generated with MA as the cross-linker through hybridization with SA and SB, followed by embedding of the AuNPs in the DNA hydrogels. When MEL was present, the specific aptamers bound with it competitively, because of the high affinity between the specific aptamers and targets, and formed target-aptamer complexes, leading to the disintegration of the DNA hydrogels and the release of the preloaded AuNPs. Visual and quantitative detection could subsequently be achieved based on the color change of the supernatant and absorbance detection. Similarly, the DNA hydrogels were placed into the designed microfluidic chips, and the unreacted DNA hydrogels blocked the liquid channel. In the presence of MEL, the DNA hydrogels gradually split and their volume reduced. The chip was tilted to make the reacted sample solution flow past the liquid channel and into the detection area by gravity, and gray value analysis was conducted based on the color change in response to the release of AuNPs, thus indicating the concentration of the target. The concentration of the target showed a positive correlation with the color depth of the reacted sample, and a negative correlation with the average gray value.

3.2. Feasibility verification

The degree of hydrogel network crosslinking was determined by the level of combination of MA and its complementary sequences. A 20% native polyacrylamide gel electrophoresis (PAGE) was employed to verify the binding of MA and its target, as well as its hybridization and de-hybridization behaviors with complementary chains. As shown in Fig. 1A, Channel a and b (chains SA and SB) differed from Channel c (MA) in molecular weight, while chains SA and SB were also clearly combined with MA (Channels d). After adding MEL, MA bands can be seen (Channel e), which proves the fracture of three complementary chains. By further increasing the concentration of MEL, it can be seen from Channel f that the three chains complex is more obviously dehybridizated.

To further verify the feasibility of the experiment, CD was employed to prove the change in conformation after binding of the complementary DNA hybrid chain and MEL to MA. As shown in Fig. 1B, MEL did not exhibit a peak showing its secondary structure, and MA was observed to have a maximum positive peak at 284 nm and a maximum negative peak at 241 nm, while the SA + SB chain exhibited a maximum positive peak at 277 nm and a maximum negative peak at 251 nm. Compared with the MA chain and the SA + SB chain, the SA + SB + MA chain had a redshift and blueshift, respectively, in the peak value, which demonstrates that MA hybridizes with its complementary chains and has an altered



Scheme 1. Schematic depicting the DNA hydrogel for melamine detection combined with microfluidic chip.

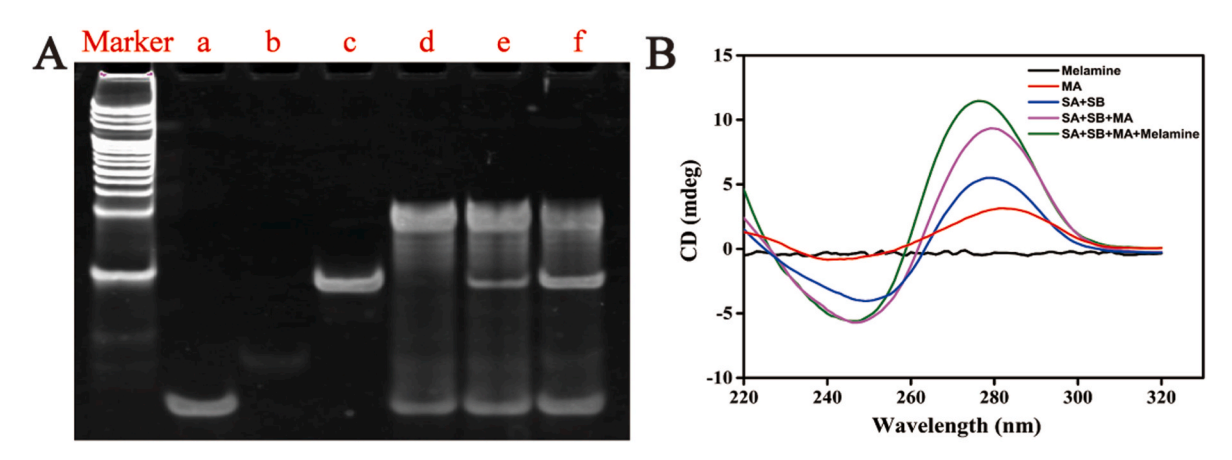


Fig. 1. Feasibility verification. (A) 20% Native-PAGE. a: SA, b: SB, c: MA, d: SA + SB + MA, e: SA + SB + MA + MEL (10 μ M), f: SA + SB + MA + MEL (100 μ M). The concentrations of SA, SB and MA are 2.0 μ M, 2.0 μ M and 1 μ M, respectively. (B) CD spectra of DNA copolymers used in this work, where the concentrations of SA, SB, MA, and MEL are 10 μ M, 10 μ M, 10 μ M, and 20 μ M, respectively.

secondary structure. An obvious redshift with an increased peak value was observed at the positive peak (277 nm) after MEL was added to the hybrid chains, showing that MEL competitively combined with MA on the hybrid chains and further changed the structure of the system.

Finally, we synthesized MEL-responsive DNA hydrogels (the volume of AuNPs added was 7 μL , and MA concentration was 40 μM) for control test. Before introducing MEL, rinse with tris HCl buffer for 3 times to remove free AuNPs, and then added MEL with concentration of 50 μM , reacted at 37 °C and 150 rpm, and took photos and records. As shown in Fig. S3, which fully proved the feasibility of the experiment.

3.3. Optimization of experimental conditions

The cross-linking degree of DNA has a direct effect on the network structure of hydrogels. After fixing the concentration of SA and Sb in the chain of the complex, in order to achieve the highest performance of the DNA hydrogel for the detection of MEL, the formation conditions, reaction time, volume of encapsulated AuNPs, and pH of the reaction system were optimized. First, the concentration of MA was optimized as

it specifically reacts with MEL as a bridging chain of the nucleic acid hydrogels and causes the disintegration of the nucleic acid hydrogels and the release of AuNPs. The dissociation dynamics of MA at different concentrations were observed by monitoring the absorbance at 524 nm (absorbance maximum of the 15 nm AuNPs). As shown in Fig. 2A-D, with an MA concentration of 30 μ M, the system gradually collapsed over time after the target was added, whereas the hydrogels also gradually dissociated as they absorbed water and swelled in the absence of the target. It is clear that the low concentration of the bridging chain resulted in a low overall cross-linking degree of the system (Fig. 2A). The cross-linking degree of the DNA hydrogels improved as MA concentration was increased to 35 µM, but the hydrogel system still gradually dissociated in the absence of MEL (Fig. 2B). When MA concentration was increased to 40 μ M, the system reaches the plateau stage when the reaction reaches 60 min, the absorbance basically does not increase, and the reaction reaches the maximum efficiency. At this time, the dissociation degree of the blank control is very low, which means that the system is stable and has high sensitivity to the target (Fig. 2C). However, the cross-linking degree of the system further improved as the MA

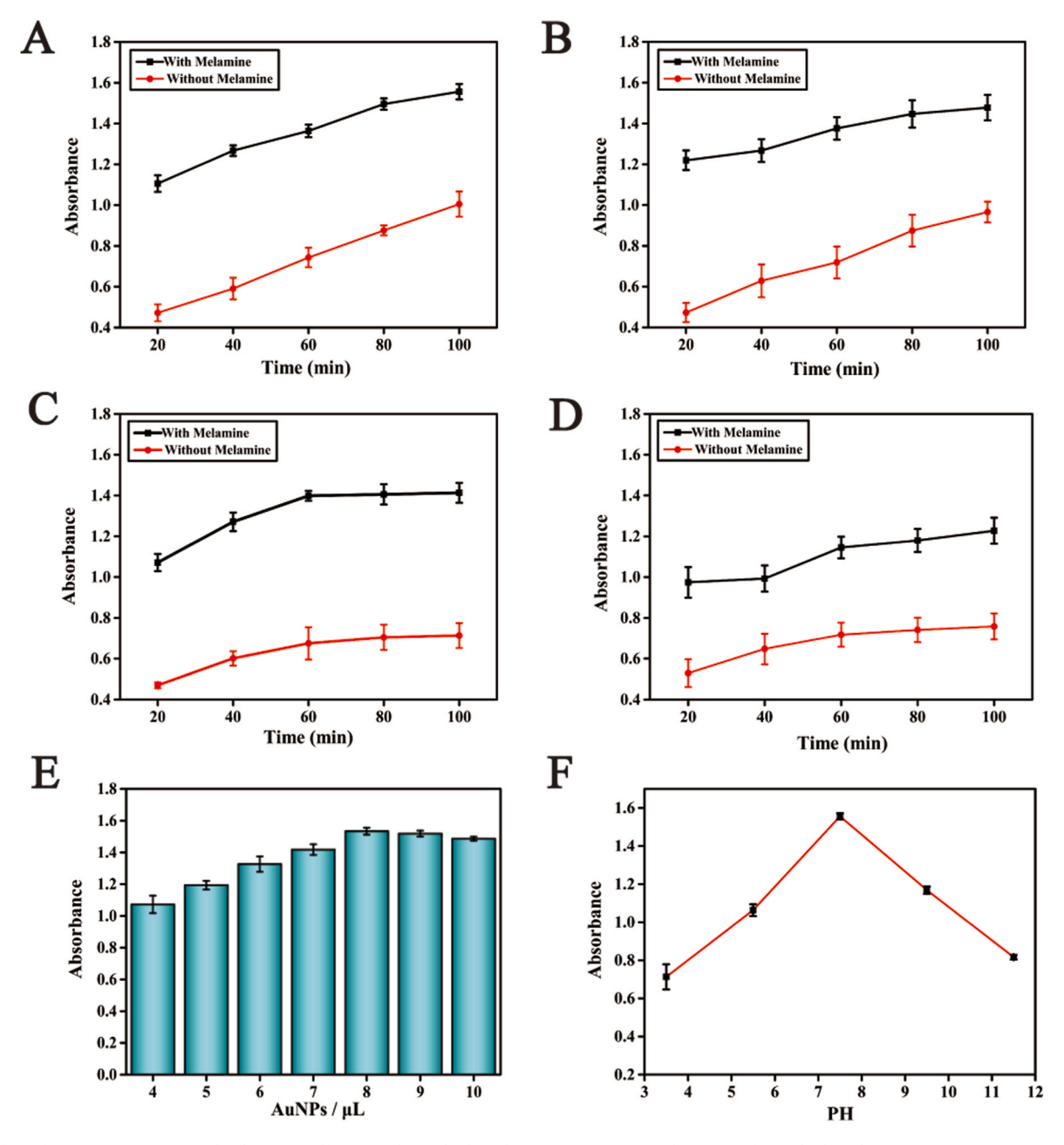


Fig. 2. Effect of MA concentration on the detection efficiency of DNA hydrogels. (A–D) Dissociation dynamics of DNA hydrogels at 524 nm at a MA concentration of 30 μ M, 35 μ M, 40 μ M and 50 μ M, respectively. (E) Effect of volume of encapsulated AuNPs on absorbance. (F) The effect of the pH on the detection of MEL. The error bars represent the standard deviations of three replicate experiments.

concentration increased to 50 $\mu M,$ making it insensitive to MEL (Fig. 2D). In conclusion, maximum efficiency was achieved 60 min after the start of the reaction with a 40 μM MA concentration.

The concentration of AuNPs was positively correlated with the color depth of the hydrogels. The AuNP concentration was set at 0.5 mg/mL to ensure successful colorimetric detection of the experimental results. The volume of AuNPs loaded in the DNA hydrogels was subsequently further optimized because the amount of encapsulated AuNPs had a profound effect on experimental sensitivity. As shown in Fig. 2E, the monitored absorbance values increased as the amount of AuNPs loaded in the DNA hydrogel increased, and reached a maximum when the embedded volume was 8 μ L. When the loading volume was increased further, the raised background signal resulted in a decreased absorbance. The comparison photos before and after the optimization conditions are shown in Fig. S4. Thus, the optimal volume of AuNPs embedded in the

DNA hydrogel was determined to be 8 µL.

Finally, the pH of the reaction system was optimized to determine optimal reaction conditions. By adjusting the pH of the supernatant, the reaction efficiency was determined at pH 3.5, 5.5, 7.5, 9.5, and 11.5. As shown in Fig. 2F, the reaction efficiency was highest when the pH value of the supernatant was 7.5.

3.4. Characterization

The optimized DNA hydrogels were observed by SEM to verify the successful synthesis of the DNA hydrogels. After freeze-drying, the DNA hydrogels were found to have a multi-hole cross-linking network in the SEM image (Fig. 3A and B), consistent with the morphology of the hydrogel matrix. Next, the synthesized DNA hydrogels were dissolved and diluted with water and characterized by TEM, and the results

showed that the AuNPs were regularly scattered in the system (Fig. 3C).

Rheological studies were conducted to further understand the physical states of the DNA hydrogels. The storage modulus (G') and loss modulus (G") of the optimized DNA hydrogels were compared to assess the ability of the compound to revert to its original geometric shape and the flow tendency of the materials. As shown in Fig. 3D, the moduli (G' and G") were slightly frequency-dependent, without crossing each other during the entire range of test frequencies, which means that the elastic response dominates, and the materials have a permanent network of high cross-linking. G" was always lower than G', suggesting the existence of gelatinous behavior in the DNA hydrogel.

3.5. Quantitative detection of the DNA hydrogels

The detection ability of the DNA hydrogel for MEL can be judged by the color of the supernatant on the one hand, and quantitatively expressed by detecting the absorbance of the supernatant on the other hand. The results shown in Fig. 4 revealed that a higher level of cleavage reactions and a decreased cross-linking degree with an increased MEL concentration, which accelerated the disintegration of the hydrogels and the subsequent release of AuNPs into the supernatant. Data from UV–vis (Fig. 4A) showed that absorbance exhibited a positive correlation with MEL concentration and the MEL at concentrations of 0.1–100 μ M exhibited a logarithmic linear correlation with the absorbance of the supernatant (Fig. 4B). The linear equation was Y = 0.1977Lg X + 1.1487. Evidently, MA was depleted in the plateaued reaction when the concentration of the MEL was further increased. The LOD of the sensor was 42 nM, obtained using the formula $3\sigma/\text{slope}$, where σ is the standard deviation of the blank sample (n = 11) and the slope represents the slope

of the linear equation (0.1977).

3.6. Specificity and anti-interference ability detection

The potential substances affecting the sensor were explored to evaluate the anti-interference performance and specificity of the sensor after confirming that the sensor responded quickly to MEL. Testing included certain substances commonly coexisting with MEL, such as glucose, sucrose, lysine, L-cysteine, histidine, adenine, and thymine. In addition, metal ions likely to affect the sensor, such as Pb^{2+} and Al^{3+} , were also included in the test panel. The detectable concentrations of these coexisting substances and metal ions were ten times higher that of MEL. The experimental results shown in Fig. 5 suggest that only MEL had a noticeable impact on the sensor under the same conditions, and the absorbance changed only slightly in response to interfering substances, signifying that the developed method of MEL detection is highly specific.

3.7. Application

To explore the applicability of the method, milk and infant milk powder were supplemented with MEL at different concentrations (Table 1). The recovery rate of practical samples was found to be 87.3–112%, and the relative standard deviation (RSD) was between 1.4 and 5.7%, demonstrating the potential of this method in monitoring MEL in milk and infant milk powder.

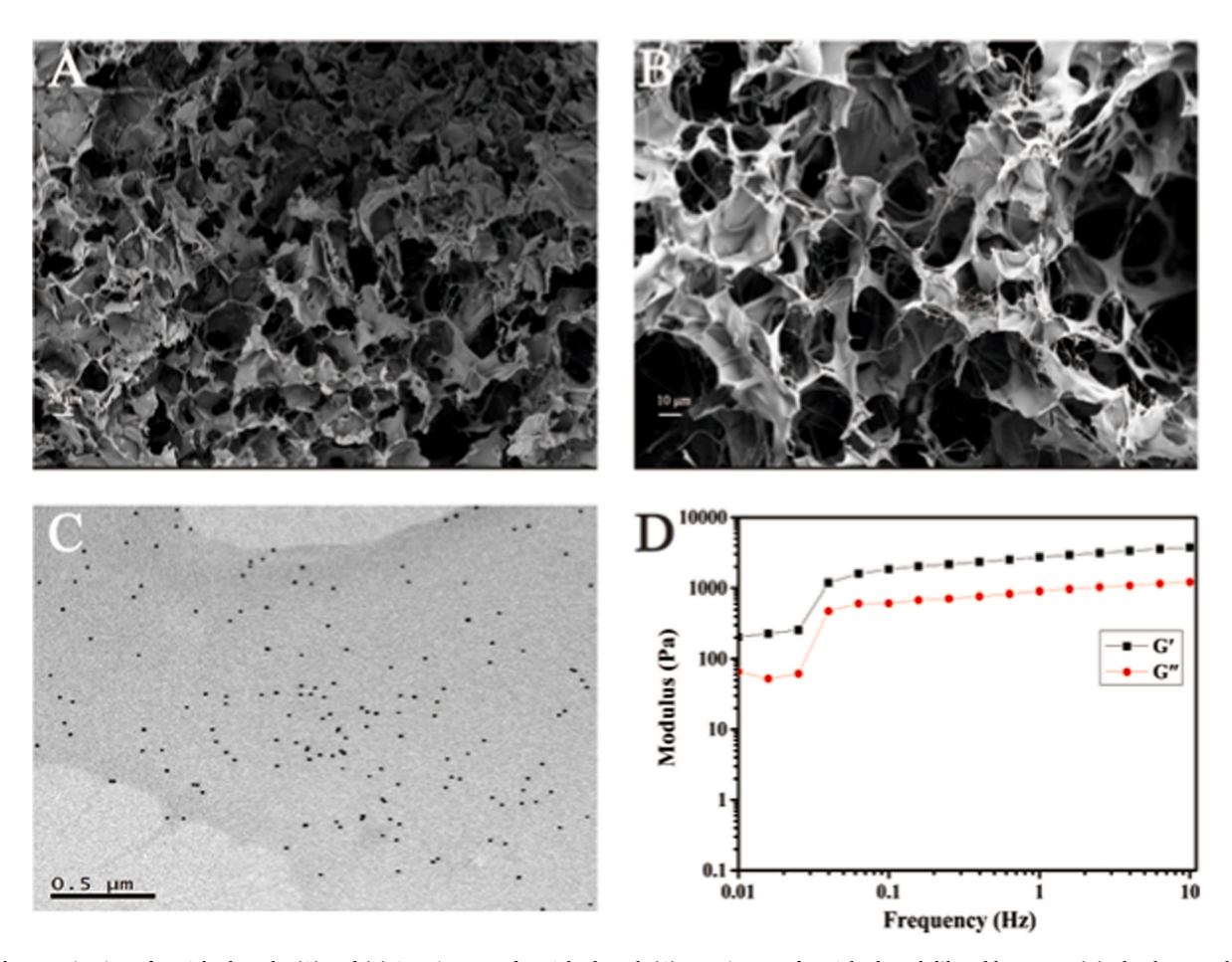


Fig. 3. Characterization of DNA hydrogels. (A) and (B) SEM images of DNA hydrogel. (C) TEM image of DNA hydrogel diluted by water. (D) Rheology studies of the DNA hydrogel.

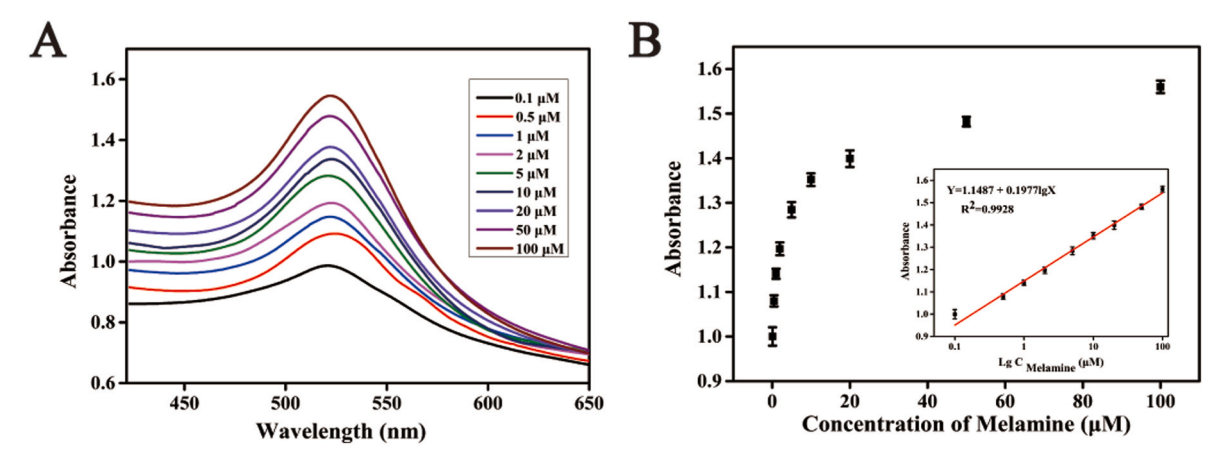


Fig. 4. Sensitivity of DNA hydrogels to MEL. (A) UV-vis absorbance spectra of the supernatant after reaction with different concentrations of MEL. (B) Standard curves of DNA hydrogels reacting with the MEL at different concentrations. The error bars represent the standard deviations of three replicate experiments.

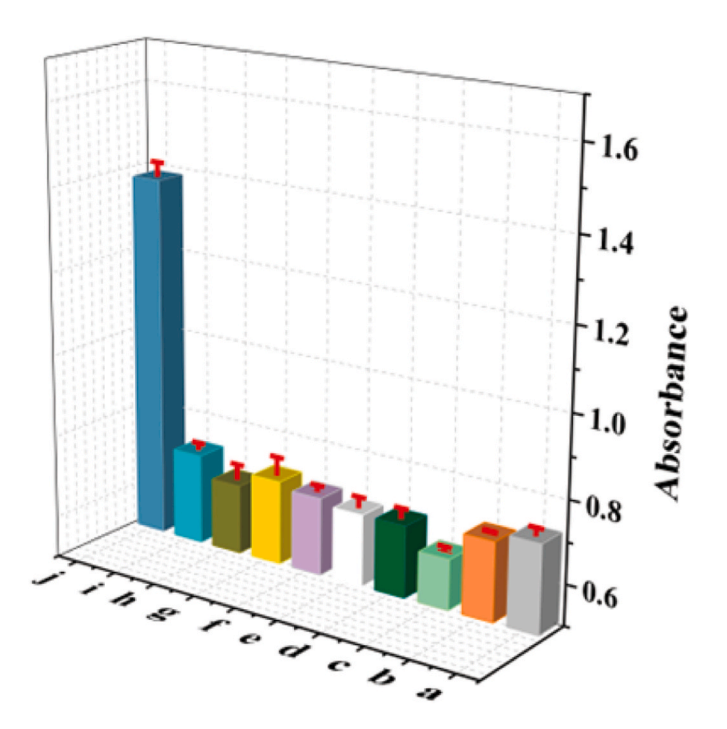


Fig. 5. Results of the selectivity of DNA hydrogel detection. a, Glucose, b. Sucrose, c. Pb^{2+} , d. Al^{3+} , e. Lysine, f. $\iota(+)$ -Cysteine, g. Histidine, h. Adenine, i. Thymine, j. MEL. (The concentration of melamine is $10~\mu M$, and the rest is 10~times higher.) The error bars represent the standard deviations of three replicate experiments.

3.8. Stability

Verifying the stability of DNA hydrogel is helpful to realize the commercialization of the detection platform. First, MEL with low, medium, and high concentrations was selected for ten repeated

Table 1 Results of MEL detection in real samples using the DNA hydrogel (n = 3).

Sample	Added (μM)	Detected(µM)	Recovery (%)	RSD (%)
Milk	0	Not detected	-	-
	10	9.80	98.0	1.4
	100	112.00	112.0	3.2
Infant milk powder	0	Not detected	-	-
	10	8.73	87.3	1.6
	100	103.03	103.0	5.7

experiments. The results are shown in Fig. 6A. The RSD is less than 2.8%, indicating that the target response DNA hydrogel has good repeatability. Furthermore, low, medium, and high concentrations of MEL standard samples were added to hydrogels stored at 4 $^{\circ}$ C, 0, 7, 14 and 21 days respectively. The results showed that the detection results at the same concentration were very similar in different days (Fig. 6B), indicating that the prepared target response DNA hydrogel was very stable.

3.9. Intuitive detection using microfluidic chips

Microfluidic chips were designed based on the characteristics of DNA hydrogels to support POCT detection and to make the detection process as economical, user-friendly, responsive, and precise as possible. After drawing patterns using AutoCAD software, microfluidic chips were prepared by Suzhou Shuotian Automation Technology Co., Ltd. (Suzhou, China) with polydimethylsiloxane (PDSM) upon receiving the patterns. Colorimetric detection was performed on the basis of the color change of the copolymerization solutions after the reaction, the copolymerization solutions after reaction were photographed using a mobile phone, and the photos were analyzed using ImageJ software to obtain aeading of the average gray value for subsequent quantitative analysis. The average gray value of the blank control group was 201. As the MEL concentration increased, the color of the copolymerization solutions flowing into the detection area of the microfluidic chips gradually deepened (Fig. 7A). Further quantitative results, shown in Fig. 7B, showed that the average gray value was linearly related to the logarithm of MEL concentration in the range of $0.2–50~\mu M$, the linear equation was Y = -20.6981 Lg X + 180.0410. The LOD of the sensor was 37 nM, obtained using the formula $3\sigma/\text{slope}$, where σ is the standard deviation of the blank sample (n = 11) and the slope represents the slope of the linear equation. Compared with previous detection methods (Table S2), the method developed in this study displayed a superior detection ability.

4. Conclusions

In this study, DNA hydrogels specifically responding to MEL were created with MA as the bridging chain, and a portable, rapid, and sensitive POCT detection platform was developed by combining the DNA hydrogels and microfluidic chips. In the presence of the target, the specific aptamer will competitively bind to it, causing a decline in the degree of crosslinking in the DNA hydrogels. Colorimetric and quantitative detection can be achieved by detecting the release of embedded AuNPs following disintegration of the DNA hydrogels. Images taken using mobile phones and analyzed using specific software can be used to achieve POCT detection, instead of using large-scale laboratory

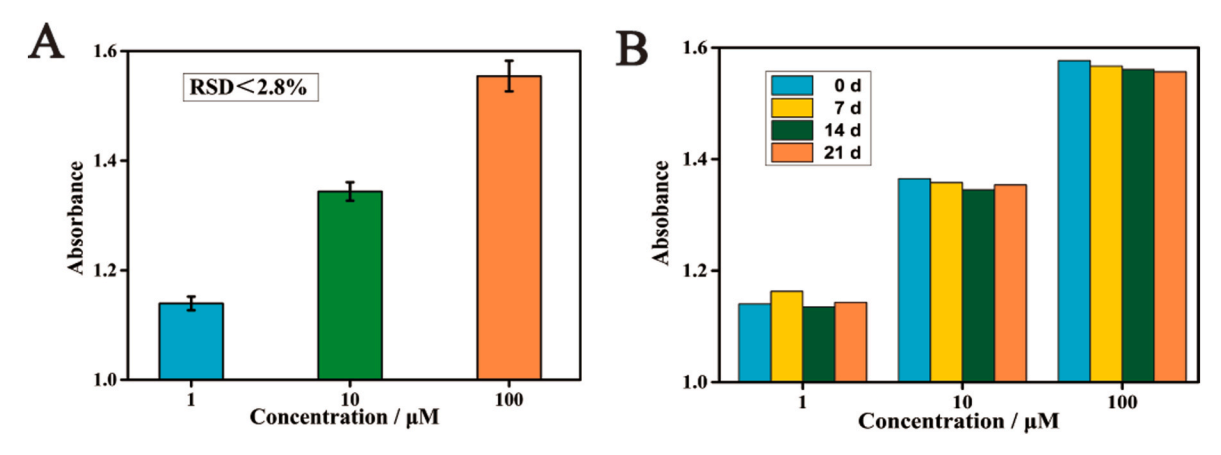


Fig. 6. Stability of DNA hydrogel for MEL detection. (A) UV–vis absorbance of the supernatant after reaction with different concentrations of MEL. The error bars represent the standard deviations of ten replicate experiments. (B) UV–vis absorbance of the supernatant after reaction with different concentrations of MEL for DNA hydrogel after 0 d, 7 d, 14 d, 21 d.

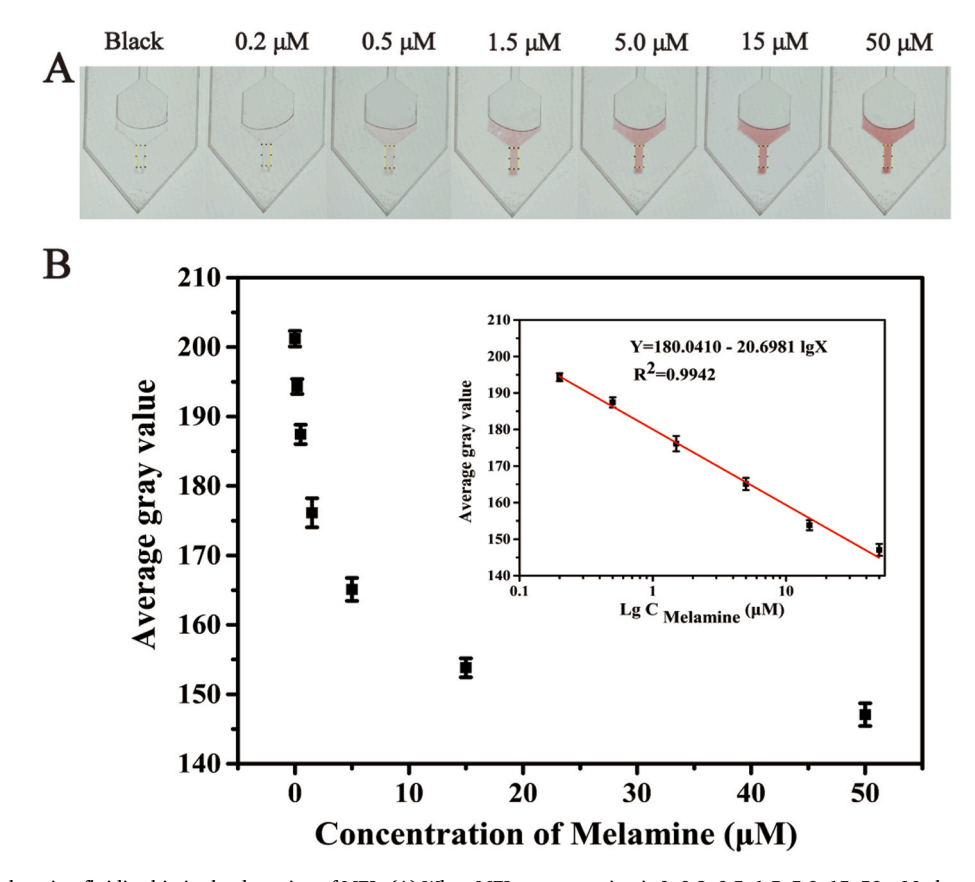


Fig. 7. Performance of the microfluidic chip in the detection of MEL. (A) When MEL concentration is 0, 0.2, 0.5, 1.5, 5.0, 15, 50 μ M, the color transformation image of the detection area of the microfluidic chip. (B) Standard curve of MEL at different concentrations detected by microfluidic chip. The error bars represent the standard deviations of three replicate experiments. (For interpretation of the references to color in this figure legend, the reader is referred to the Web version of this article.)

instruments. The platform does not require specifically trained personnel for proper application, and the determined LOD of 37 nM is lower than the limit of 0.15 mg ${\rm kg}^{-1}$ MEL in liquid infant formula specified by the international Codex Alimentarius Commission. The developed DNA hydrogels with excellent response specificity and anti-interference ability showed no apparent response to other substances. The results showed a MEL recovery rate 87.3–112% in milk and infant milk powder, with an RSD of 1.4–5.7%. In addition, the high specificity and responsiveness of aptamers to their targets gives this method potential for application in the portable quantitative detection of various

targets by changing the aptamers and designing the complementary sequence of response. In conclusion, we developed a user-friendly POCT device based on MEL-responsive DNA hydrogels and microfluidic chips, which is simple to operate, portable, and uses mobile phones for analyzing the results without relying on other devices. The proposed method has high potential for application in food safety analysis and medical diagnostics. Our future studies will be aimed at making the method more intelligent.

CRediT authorship contribution statement

Zhiguang Wang: Conceptualization, Data curation, Writing – original draft. Ruipeng Chen: Writing – review & editing. Yue Hou: Methodology. Yingkai Qin: Software. Shuang Li: Formal analysis, Funding acquisition. Shiping Yang: Supervision. Zhixian Gao: Supervision, Project administration.

Declaration of competing interest

The authors declare that they have no known competing financial interests or personal relationships that could have appeared to influence the work reported in this paper.

Data availability

Data will be made available on request.

Acknowledgments

National key research and development program (2021YFA0910204) and Key science and technology project of Henan Province (222102310514) for funding this research project.

Appendix A. Supplementary data

Supplementary data to this article can be found online at https://doi.org/10.1016/j.aca.2022.340312.

References

- [1] J. Li, X. Gao, Y. He, L. Wang, Y. Wang, L. Zeng, Elevated emissions of melamine and its derivatives in the indoor environments of typical e-waste recycling facilities and adjacent communities and implications for human exposure, J. Hazard Mater. 432 (2022), 128652.
- [2] L. Finete Vde, M.M. Gouvêa, F.F. Marques, A.D. Netto, Is it possible to screen for milk or whey protein adulteration with melamine, urea and ammonium sulphate, combining Kjeldahl and classical spectrophotometric methods? Food Chem. 141 (2013) 3649–3655.
- [3] C.F. Nascimento, P.M. Santos, E.R. Pereira-Filho, F.R.P. Rocha, Recent advances on determination of milk adulterants, Food Chem. 221 (2017) 1232–1244.
- [4] R.P. Dalal, D.S. Goldfarb, Melamine-related kidney stones and renal toxicity, Nat. Rev. Nephrol. 7 (2011) 267–274.
- [5] C.C. Liu, T.J. Hsieh, C.F. Wu, C.H. Lee, Y.C. Tsai, T.Y. Huang, S.C. Wen, C.H. Lee, T. M. Chien, Y.C. Lee, S.P. Huang, C.C. Li, Y.H. Chou, W.J. Wu, M.T. Wu, Interrelationship of environmental melamine exposure, biomarkers of oxidative stress and early kidney injury, J. Hazard Mater. 396 (2020), 122726.
- [6] Y. Lu, Y. Xia, G. Liu, M. Pan, M. Li, N.A. Lee, S. Wang, A review of methods for detecting melamine in food samples, Crit. Rev. Anal. Chem. 47 (2017) 51–66.
- [7] C. Hazra, V.N. Adusumalli, V. Mahalingam, 3,5-Dinitrobenzoic acid-capped upconverting nanocrystals for the selective detection of melamine, ACS Appl. Mater. Interfaces 6 (2014) 7833–7839.
- [8] X. Liao, C. Chen, P. Shi, L. Yue, Determination of melamine in milk based on β-cyclodextrin modified carbon nanoparticles via host-guest recognition, Food Chem. 338 (2021), 127769.
- [9] L. Xie, X. Zi, H. Zeng, J. Sun, L. Xu, S. Chen, Low-cost fabrication of a paper-based microfluidic using a folded pattern paper, Anal. Chim. Acta 1053 (2019) 131–138.

- [10] L. Fabiani, V. Mazzaracchio, D. Moscone, S. Fillo, R. De Santis, A. Monte, D. Amatore, F. Lista, F. Arduini, Paper-based immunoassay based on 96-well waxprinted paper plate combined with magnetic beads and colorimetric smartphoneassisted measure for reliable detection of SARS-CoV-2 in saliva, Biosens. Bioelectron. 200 (2022), 113909.
- [11] F. Lisi, J.R. Peterson, J.J. Gooding, The application of personal glucose meters as universal point-of-care diagnostic tools, Biosens. Bioelectron. 148 (2020), 111835.
- [12] T. Guan, Z. Xu, J. Wang, Y. Liu, X. Shen, X. Li, Y. Sun, H. Lei, Multiplex optical bioassays for food safety analysis: toward on-site detection, Compr. Rev. Food Sci. Food Saf. 21 (2022) 1627–1656.
- [13] N.H. Bhuiyan, J.H. Hong, M.J. Uddin, J.S. Shim, Artificial intelligence-controlled microfluidic device for fluid automation and bubble removal of immunoassay operated by a smartphone, Anal. Chem. 94 (2022) 3872–3880.
- [14] S. Ohta, R. Hiraoka, Y. Hiruta, D. Citterio, Traffic light type paper-based analytical device for intuitive and semi-quantitative naked-eye signal readout, Lab Chip 22 (2022) 717–726.
- [15] Y. Xie, X. Wei, Q. Yang, Z. Guan, D. Liu, X. Liu, L. Zhou, Z. Zhu, Z. Lin, C. Yang, A Shake&Read distance-based microfluidic chip as a portable quantitative readout device for highly sensitive point-of-care testing, Chem. Commun. 52 (2016) 13377-13380
- [16] Z. Zhu, Z. Guan, S. Jia, Z. Lei, S. Lin, H. Zhang, Y. Ma, Z.Q. Tian, C.J. Yang, Au@Pt nanoparticle encapsulated target-responsive hydrogel with volumetric bar-chart chip readout for quantitative point-of-care testing, Angew. Chem. 53 (2014) 12503–12507.
- [17] M. Marin, M.V. Nikolic, J. Vidic, Rapid point-of-need detection of bacteria and their toxins in food using gold nanoparticles, Compr. Rev. Food Sci. Food Saf. 20 (2021) 5880–5900.
- [18] J.S. Kahn, Y. Hu, I. Willner, Stimuli-responsive DNA-based hydrogels: from basic principles to applications, Acc. Chem. Res. 50 (2017) 680–690.
- [19] F. Huang, M. Chen, Z. Zhou, R. Duan, F. Xia, I. Willner, Spatiotemporal patterning of photoresponsive DNA-based hydrogels to tune local cell responses, Nat. Commun. 12 (2021) 2364.
- [20] C. Wang, X. Liu, V. Wulf, M. Vázquez-González, M. Fadeev, I. Willner, DNA-based hydrogels loaded with Au nanoparticles or Au nanorods: thermoresponsive plasmonic matrices for shape-memory, self-healing, controlled release, and mechanical applications, ACS Nano 13 (2019) 3424–3433.
- [21] X. Ma, Z. Yang, Y. Wang, G. Zhang, Y. Shao, H. Jia, T. Cao, R. Wang, D. Liu, Remote controlling DNA hydrogel by magnetic field, ACS Appl. Mater. Interfaces 9 (2017) 1995–2000.
- [22] W. Xu, Y. Huang, H. Zhao, P. Li, G. Liu, J. Li, C. Zhu, L. Tian, DNA hydrogel with tunable pH-responsive properties produced by rolling circle amplification, Chemistry 23 (2017) 18276–18281.
- [23] Y. Gu, M.E. Distler, H.F. Cheng, C. Huang, C.A. Mirkin, A general DNA-gated hydrogel strategy for selective transport of chemical and biological cargos, J. Am. Chem. Soc. 143 (2021) 17200–17208.
- [24] X. Ji, H. Lv, X. Sun, C. Ding, Green-emitting carbon dot loaded silica nanoparticles coated with DNA-cross-linked hydrogels for sensitive carcinoembryonic antigen detection and effective targeted cancer therapy, Chem. Commun. 55 (2019) 15101–15104.
- [25] W.C. Liao, S. Lilienthal, J.S. Kahn, M. Riutin, Y.S. Sohn, R. Nechushtai, I. Willner, pH- and ligand-induced release of loads from DNA-acrylamide hydrogel microcapsules, Chem. Sci. 8 (2017) 3362–3373.
- [26] H. Xiong, L. Liu, Y. Wang, H. Jiang, X. Wang, Engineered aptamer-organic amphiphile self-assemblies for biomedical applications: progress and challenges, Small 18 (2022), e2104341.
- [27] C. Gu, Y. Xiang, H. Guo, H. Shi, Label-free fluorescence detection of melamine with a truncated aptamer, Analyst 141 (2016) 4511–4517.
- [28] S. Ohta, E. Kikuchi, A. Ishijima, T. Azuma, I. Sakuma, T. Ito, Investigating the optimum size of nanoparticles for their delivery into the brain assisted by focused ultrasound-induced blood-brain barrier opening, Sci. Rep. 10 (2020), 18220.
- [29] P. Wu, S. Li, X. Ye, B. Ning, J. Bai, Y. Peng, L. Li, T. Han, H. Zhou, Z. Gao, P. Ding, Cu/Au/Pt trimetallic nanoparticles coated with DNA hydrogel as target-responsive and signal-amplification material for sensitive detection of microcystin-LR, Anal. Chim. Acta 1134 (2020) 96–105.